IAC-13,C1,4,11,x16601

AUTONOMOUS GNC FOR ASTEROID DEFLECTION AND ATTITUDE CONTROL VIA LASER ABLATION

Massimo Vetrisano
PhD Candidate, University of Strathclyde, UK, massimo.vetrisano@strath.ac.uk

Massimiliano Vasile
Professor, University of Strathclyde, UK, massimiliano.vasile@strath.ac.uk

This paper presents an autonomous guidance, navigation and control system for the deflection and attitude control of a small asteroid via laser ablation. Laser ablation consists of irradiating the surface of the asteroid with a laser beam with sufficient intensity to sublimate the irradiated material. The resulting jet of gas and debris induces a force and a torque thrusting the asteroid off its natural course and changing its tumbling motion. In this paper it is proposed to use the laser to first de-tumble the asteroid. A reduction of the rotational speed of the asteroid increases the yield of the laser ablation process. An autonomous proximity control system is then implemented to keep the spacecraft flying in formation with the asteroid under the effect of the thrust acting on the asteroid, plume impingement, laser recoil and solar radiation pressure.

The spacecraft employs and processes the measurements coming from its own on board measurements, given by a laser range finder, high resolution cameras, and an impact sensor. The latter is combined with the attitude information and, thus, used to estimate the plume impingement force, which acts in the same direction of the exerted thrust due the laser ablation. In this way the spacecraft is able to estimate on-board the imparted acceleration and the effectiveness of the laser ablation procedure. An unscented Kalman filter is used to estimate spacecraft position and velocity together with the perturbative accelerations. A second filter is implemented to estimate the asteroid's rotation by extracting and tracking the motion of asteroid's features, using either optical flow or spectral methods. These variables are used to implement spacecraft trajectory control in order to permit the laser to work at his optimal focussing distance.

Two trajectory control strategies are considered: in the first one, a series of impulse bits maintains the spacecraft within a 0.5 m box from the reference trajectory; the second strategy is based on a continuous low-thrust control. It is shown that both techniques are viable and accurate. The discrete impulsive control does not downgrade the laser performance given the small oscillations with respect to the nominal conditions. Nonetheless low thrust allows the spacecraft to impart a higher momentum onto the asteroid.

.

Keywords: Asteroid Deflection, GNC, Minor Body Proximity, Autonomy

I. ACRONYMS

AU – Astronautical Unit
CoM - Centre of Mass
FFT - Fast Fourier Transform
GNC - Guidance Navigation & Control
NEO – Near Earth Object
MOID – Minimum Orbital Intersection Distance
PHA – Potentially Hazardous Asteroids
RCS - Reaction Control System
UKF – Unscented Kalman Filter

II. INTRODUCTION

Near Earth Objects (NEO), the majority of which are asteroids, are defined as any minor celestial object with a perihelion less than 1.3 AU and an aphelion greater than 0.983 AU. A subclass of these, deemed potentially hazardous asteroids (PHA), are defined as those with a Minimum Orbital Intersection Distance (MOID) from the Earth's orbit less than or equal to 0.05 AU and a diameter larger than 150 m. As of 3rd of September 2013, 10040 NEOs have been detected; of those, more than 2900 have a diameter between 0.3 and 1 km, and 1420 are listed as PHA[1]. Impacts from asteroids of about 1 km or more in diameter are considered to be capable of causing global climate change and the destruction of ozone, with a land destruction area equivalent to a large state or country. Those with an average diameter of 100 m can cause significant tsunamis and/or the land destruction of a large city. It is estimated that there are between 30000–300000 NEOs with diameters around 100 m, meaning a large number of NEOs are still undetected.

There is wide interest in the asteroid risks mitigation. Different deflection techniques can be divided into two genres [2,3]: contact and contactless. Both the methods are valid, but contact deflection techniques, in the case of impactor, are not effective for every kind

of asteroid, such the rubble-pile ones. Moreover this solutions require an object (either a spacecraft/ man-made impactor or another asteroid) to impact the asteroid with high relative velocity. In the likely event the asteroid trajectory is not precisely known, approaching the asteroid fast will reduce the possibility to impact and impart the desired momentum. Other contact techniques which foresee to capture the asteroid and drag it on safer trajectories are difficult to scale-up to larger asteroid missions. Contactless systems are considered in general to be more flexible from this point-of-view; the approach to the asteroid is slower and the deflective action precisely controllable. Laser ablation consists of irradiating the asteroid's surface with a laser beam. The absorbed energy increases the temperature of the spot, thus the rock is brought to sublimate, transforming directly from a solid to a gas. The ablated material then expands to form a plume of ejecta which converts the thermal energy into momentum, pushing the asteroid away from its original trajectory.

In 2012 the European Space Agency (ESA) addressed a technology reference study concerning space mission concepts. The call intended to enable the modification of the orbital dynamics of a 130 tonnes meter-sized asteroids via a suitable contactless deflection technique. The mission is meant to be launch after 2025, and to have a maximum lifetime of 3 years to impart the asteroid with an overall deviation of 1 m/s. LightTouch2 mission, a consortium, led by University of Strathclyde and formed with partners from EADS Astrium Stevenage, GMV Portugal and the University of Southampton, has been selected to prove the laser ablation proof-of-concept and the feasibility of its in-space demonstration.

The results of this work[4]shows, though, that the laser requires the spacecraft to maintain a close formation at 50 m with the asteroid either along the along track or cross track direction. The laser has limited focusing capability and the plume of ejecta tends to contaminate the solar arrays, thus reducing the power available during the mission. Big variation with respect to the optimal distance could reduce dramatically process performance. With asteroids in the range of a few metres in diameter, stable terminator orbits do not exist, therefore, instead of controlling the spacecraft around a stable terminator orbit, the GNC needs to counter-act the effect of SRP to remain at the required relative position. Even if at 50 m operational distance the asteroid barely attracts the spacecraft, during ablation the spacecraft is subject to the small but not negligible perturbative force for which the spacecraft needs constantly to change its state of motion. An active control is then required to maintain the formation within a suitable operational distance. Two alternatives have been considered to control the spacecraft: a discrete control and a continuous control. The former method uses impulse bits from the RCS thrusters; the latter employs low thrust engines.

Moreover the rotation of the asteroid affects the efficiency of the whole process. [2,5] showed that the higher is the angular velocity, the lower is the imparted acceleration on the asteroid. It is, then, important to precisely point the laser on the asteroid, and possibly reduce this quantity.

Also the navigation in close proximity of asteroids can be complicated due to the fact that the environment and the response to the ablation are relatively unknown and the dynamics is highly non-linear. Thus it is necessary to estimate not only spacecraft relative trajectory but also the effects of the laser on the asteroid. This is also vital for the controlling the spacecraft around the 50m operating distance.

In this paper we consider a 600 kg spacecraft with 7.4m^2 solar arrays flying along track at 50m from the asteroid as one of the case in [4]. The asteroid trailing configuration has been chosen because it is the most effective from the deflection point of view. Also it reduces the contamination effects from the plume.

Section III describes thoroughly the proximity spacecraft and asteroid dynamics. Section III.II explains the implemented control strategy. In particular it describes spacecraft control using impulsive and continuous thrust techniques. Asteroid rotating dynamics and control are then introduced and shown in Section IV. Section V explains the set of sensors available for determining all the variables necessary to perform navigation. Section V.II is devoted to the optical flow method, which is necessary to determine the asteroid instantaneous angular velocity, which is vital to quantify the desired control torque in Section IV. Section VI describes the implemented technique for estimating the perturbative accelerations due to the interaction of the laser with the asteroid. Eventually results for both the spacecraft control strategies are shown in Section VII. Conclusions are, then, drawn in Section VIII.

III. DYNAMICS AND CONTROL

The spacecraft is required to fly in formation with the asteroid during the ablation process. The control of the ablation process requires an approximated knowledge of the distance between the laser source and the surface of the asteroid. Hence the relative position of the spacecraft needs to be determined and controlled within a given range.

III.I Proximity Motion and Perturbations

The dynamic motion of the spacecraft in the rotating Hill reference frame. In the proximity of the asteroid,

the spacecraft is subject to the resulting force due to solar pressure, the gravity of the asteroid, the gravity of the Sun, the centrifugal and Coriolis forces plus other forces induced by the impingement with the plume. Moreover the asteroid is accelerating under the effect of the laser ablation, and, thus, the spacecraft experiences the same acceleration in magnitude but in the opposite direction.

Following the ellipsoidal asteroid model, we assume that the semi-axis *c* is aligned with the z-axis of the asteroid Hill frame A (see Figure 1) at initial time.

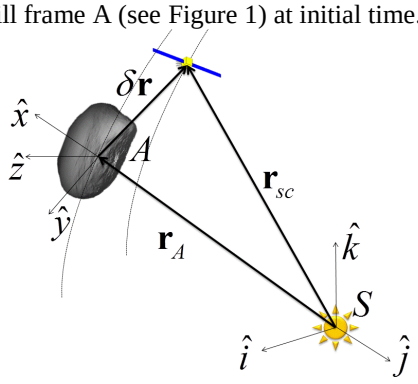

Figure 1. Definition of the reference frames, including the rotating Hill frame A centred on the asteroid.

Assuming the asteroid's shape is an ellipsoid, the gravity field of the asteroid is expressed as the sum of a spherical field plus a second-degree and second-order field [6]

$$U_{20+22} = \frac{\mu_A}{\delta r^3}\left(C_{20}(1-\frac{3}{2}\cos^2\gamma) + 3C_{22}\cos^2\gamma\cos 2\lambda \right) \quad [1]$$

where the harmonic coefficients C_{20} and C_{22} are a function of the semi-axes,

$$C_{20} = -\frac{1}{10}(2c_l^2 - a_l^2 - b_l^2)$$
$$C_{22} = \frac{1}{20}(a_l^2 - b_l^2) \quad [2]$$

and γ is defined as

$$\lambda = \arctan(\frac{y}{x}) + w_A \quad [3]$$

If one considers a Hill reference frame centred in the barycentre of the asteroid, the motion of the spacecraft in the proximity of the asteroid itself is given by [7]:

$$\ddot{\mathbf{x}} = -\mathbf{a}_{r_a} - 2\boldsymbol{\nu}\times\dot{\mathbf{x}} - \dot{\boldsymbol{\nu}}\times\mathbf{x} - \boldsymbol{\nu}\times(\boldsymbol{\nu}\times\mathbf{x}) - \frac{\mu_{sun}}{r_{Sc}^3}(\mathbf{x}+\mathbf{x}_{r_a}) - \frac{\mu_a}{\delta r^3}\mathbf{x} + \nabla U + \frac{\mathbf{F}_{sc}(\mathbf{x},\mathbf{x}_{r_a})}{m_{sc}} \quad [4]$$

where $\mathbf{a}_{r_a}$ is the projection into the local axes of the acceleration the asteroid $\ddot{\mathbf{r}}_a$ is subjected to

$$\ddot{\mathbf{r}}_a = -\frac{\mu_{sun}}{r_a^3}\mathbf{r}_a - \frac{\mu_{Sc}}{\delta r^3}\mathbf{x}_a + \mathbf{a}_{laser}$$

The second component on the right side of Eq. [4] represents the tugging effect exerted by the spacecraft on the asteroid, and $\mathbf{a}_{laser} = f(P_{available}, m_{asteroid}, A_{spot}, composition, kinematics)$ is the thrust due to the laser ablation process which depends on available power at the laser beam $P_{available}$, area of the spot on the asteroid A_{spot}, asteroid's mass, composition and kinematics [4]; $\boldsymbol{\nu}$ is the angular velocity with which the reference frame moves, and it is also affected by the process. In local reference frame its dynamics is given by

$$\mathbf{x}_{r_a}\times(\dot{\boldsymbol{\nu}}\times\mathbf{x}_{r_a}) + 2\dot{\mathbf{x}}_{r_a}\times(\boldsymbol{\nu}\times\mathbf{x}_{r_a}) = \mathbf{x}_{r_a}\times\mathbf{a}_{laser-local} \quad [5]$$

being $\mathbf{a}_{laser-local}$ is the projection of $\mathbf{a}_{laser}$ into the local reference frame. $\mathbf{F}_{sc}(\mathbf{x},\mathbf{x}_{r_a})$ includes all the perturbations due to solar radiation pressure, the laser recoil and plume impingement [8]:

$$F_{Solar} = C_R S_{srp}\left(\frac{r_{AU}}{r_{sc}}\right)^2 A_M \frac{\mathbf{x}_a}{r_{Sc}}$$
$$F_{recoil} = \eta_{sys} S_{srp}\left(\frac{r_{AU}}{r_{sc}}\right)^2 A_M \frac{\mathbf{x}}{\delta r} \quad [6]$$
$$F_{plume} = \rho_{plume}(\delta r)\bar{v}_{plume}^2(\delta r) A_{eq}\frac{\mathbf{x}}{\delta r}$$

where C_R is the reflectivity coefficient and S_{srp} is the solar flux at 1 AU, A_M is the area of the solar arrays, A_{eq} is the spacecraft cross section for the plume impingement, ρ_{plume} and $\bar{v}_{plume}$ are respectively the plume's density and velocity at the spacecraft (dependant on the distance from the spot [4]. The motion of the spacecraft is thus ruled by:

- Laser recoil: Reaction force induced by conservation of momentum upon the projection of laser photons. This force acts to push the spacecraft away from the asteroid.
- Solar radiation pressure: exerted mainly in the 7.4 m^2 solar panels, but also partially in the spacecraft body. The spacecraft is nominally sun pointing, but the nominal value still changes with the distance to the Sun. A part from that, it can be considered a stochastic value where the magnitude changes by 20% (conservative) with respect to its nominal.
- Plume impingement: Caused by the jet of ejecta plume hitting the body and solar panels of the spacecraft. Pushes the spacecraft away from the

asteroid. The magnitude depends on the cross section of the exposed surface.

- Deflection induced: a fictitious force arising from the accelerating local frame. The frame is centred in the asteroid's Centre of Mass (CoM), which is, through ablation, thrusting with a 10 mN force, thus accelerating at 0.077 μm/s2. The chase caused by this acceleration is equivalent to a force, when seen in a local frame of about 42μN.

III.II Spacecraft Control

The GNC needs to estimate the distance of the laser from the surface of the asteroid and the distance of the spacecraft from its CoM. In order to focus the beam onto the surface, the laser-to-surface distance must be known with a0.1m accuracy to limit the complexity of the optics. Trajectory estimation is performed by combining information from the on board camera and LIDAR Range Finder, along with the measurements from the opportunistic payload, i.e. impact sensor and spectrometer [4]. The ranging sensors directly measure this quantity, more specifically the range in the direction of the beam's boresight. Combining with Line Of Sight (LOS) measurements, this can directly be converted to altitude, that is, range to surface in the SC-CoM direction. The spacecraft-to-CoM distance is is the quantity of interest to control the translational dynamics. Figure 2 shows how rotation is coupled with the measurements.

The implications for GNC are numerous: on one hand, a measurement is available that (with little filtering) can provide cm accuracy to focus the beam. On the other hand the translational control cannot react to keep this measurement constant, because that would imply a large amount of actuations. Furthermore, the spacecraft determines its trajectory with respect to the CoM, so it would be easier to refer to the spacecraft relative position rather than to the range from th surface.

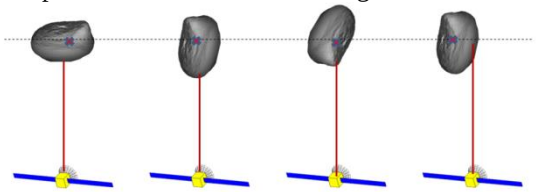

Figure 2. Range to surface change with rotation of the asteroid

To provide insight to this issue, consider the 2 DoF simplification shown in Figure 3. The asteroid has been assumed to be an ellipsoid with semi-axes given $[a \quad b \quad c] = [2.3 \quad 3.0 \quad 1.5]m$. Being the difference between the maximum and minimum axis of the ellipsoid equal to 1.5m, the rotation of the asteroid, at maximum, will cause an excursion in range of ±1.5 m , if the CoM distance remains fixed. The focusing of the laser is such that the distance beyond which the defocusing of the laser beam would stop the ablation process is close to ±2 m about the nominal operating distance. Translated to a requirement, this means that the CoM distance needs to be controlled to a box of ±0.5 m. Figure 3 shows how an excursion of ±0.5 m in CoM plus the rotation lead to an excursion of range to surface of ±2 m.

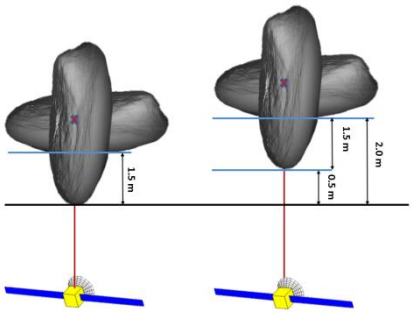

Figure 3. Maximum excursion of range to surface caused by a 2 m excursion in CoM range and rotation

Two control logics have been implemented for the formation. The first one is a discrete limit cycle control based on impulsive bits from RCS thrusters. The second employs a continuous thrust to constantly maintain the spacecraft within the box.

Discrete Control

At each instant of time the autonomous system propagates the estimated state up to the following instant of time. Then the system checks for the inclusion of the spacecraft between the boundaries defined by the control box. The control allocates an impulse bit, keeping into account the estimated acceleration acting on that direction, exploiting the dynamics to reduce the overall number of actuations. It is assumed that within the control box the total acceleration acting on the spacecraft is constant. Under the effect of a constant acceleration, the motion of the spacecraft within the control box is given by:

$$\mathbf{d} = \mathbf{d}_{in} + (\mathbf{v}_{in} + \Delta\mathbf{v}_{corr})t + \mathbf{a}_{est}\frac{t^2}{2} \qquad [7]$$

where $\mathbf{d}_{in}$ and $\mathbf{v}_{in}$ are the initial position and velocity error with respect to the nominal trajectory, $\Delta\mathbf{v}_{corr}$ is the corrective impulse bit, while $\mathbf{a}_{est}$ is the acceleration acting on the spacecraft. The corrective impulse bit is allocated such that the spacecraft reaches the other side of the control box, with relative velocity equal to 0.

$$\mathbf{v}_{in}^{est} + \Delta\mathbf{v}_{corr} + \mathbf{a}_{est} t = 0$$
$$\mathbf{d}_f = \mathbf{d}_{in}^{est} + (\mathbf{v}_{in}^{est} + \Delta\mathbf{v}_{corr})t + \mathbf{a}_{est}\frac{t^2}{2} \quad [8]$$

where position and velocity have been substituted by their estimated counterpart at the current instant of time. In order to achieve this limit cycle, an estimate of the relative acceleration is necessary.

Continuous Control

If one assumes that centrifugal and Coriolis forces are negligible compared to solar pressure, gravity of the asteroid, and plume and that any non-spherical terms in the gravity field expansion results in only a small perturbation, then one can build a simple control law based on the Lyapunov control function[8]:

$$V = \frac{1}{2}\delta v^2 + \frac{1}{2}K\left(\left(x - x_{ref}\right)^2 + \left(y - y_{ref}\right)^2 + \left(z - z_{ref}\right)^2\right) \quad [9]$$

where $\delta\mathbf{r}_{ref} = [x_{ref} \quad y_{ref} \quad z_{ref}]$ are the coordinates of a point along the nominal formation orbit (in the Hill frame). The assumption here is that the motion along the reference formation orbit is much slower than the control action.

The necessary condition for the stability of the controller is that it must exist a controller **u** such that $dV/dt < 0$. Such a controller is defined as follows:

$$\mathbf{u} = -\left(\mathbf{a}_{Sun}(\delta\mathbf{r}) - \frac{\mu_A}{\delta r^3}\delta\mathbf{r}\right) - K\left(\delta\mathbf{r} - \delta\mathbf{r}_{ref}\right) - c_d\delta\mathbf{v} \quad [10]$$

If the actual trajectory of the spacecraft was known, the continuous control in Eq.[10] can now be introduced into the full dynamics model in Eqs.. Though, the trajectory is estimated by the navigation and in this way Eq.[10] becomes:

$$\mathbf{u} = -\left(\mathbf{a}_{Sun}(\delta\mathbf{r}_{est}) - \frac{\mu_A}{\delta r^3}\delta\mathbf{r}\right) - K(t)\left(\delta\mathbf{r}_{est} - \delta\mathbf{r}_{ref}\right) - c_d(t)\delta\mathbf{v}_{est} \quad [11]$$

where $\delta\mathbf{r}_{ref}$, $\delta\mathbf{v}_{ref}$ are the estimated position and velocity from the filter and the two coefficients are time dependant, in order to account for the filter to converge, thus reducing initial control. The elastic coefficient *K* was chosen to have $10^{-5}/s^2$ as steady value while the steady dissipative coefficient c_d was set to $10^{-3}/s$.

IV ASTEROID ROTATIONAL DYNAMICS AND CONTROL

Given the fact that the yield of the laser ablation process is higher when the angular velocity of the asteroid is lower, decreasing its angular velocity by pointing the laser off-barycentre can increase the process effectiveness. Thus the desired deflection can be achieved in a shorter time, or, conversely, higher deflection can be obtained in a year operations. The dynamics of the rotating body is given by a set of 7 differential equations, which describes the evolution of the asteroid attitude, here represented by quaternions, and its angular velocity :

$$\dot{\mathbf{q}} = \frac{1}{2}\mathbf{\Omega}\mathbf{q}$$
$$\mathbf{I}\dot{\boldsymbol{\omega}} + \boldsymbol{\omega} \times \mathbf{I}\boldsymbol{\omega} = \mathbf{M}_c \quad [12]$$

where $\mathbf{q} = [q_1 \quad q_2 \quad q_3 \quad q_4]$ is the quaternions array, $\omega = [\omega_x \quad \omega_y \quad \omega_z]$ is the angular velocity array in the inertial reference frame, I is matrix of inertia of the asteroid; $\mathbf{M}_c$ is the control momentum, and $\mathbf{\Omega}$ is given by

$$\mathbf{\Omega} = \begin{bmatrix} 0 & \omega_z & -\omega_y & \omega_x \\ -\omega_z & 0 & \omega_x & \omega_y \\ \omega_y & -\omega_x & 0 & \omega_z \\ -\omega_1 & -\omega_y & -\omega_z & 0 \end{bmatrix} \quad [13]$$

It has to be pointed out that we neglected the perturbative torque because the overall effect is negligible with respect to the torque induced by the laser, and also we did not consider the contribution given by the rotation around the Sun (equal to $2\pi/T_a \approx 1.9\cdot10^{-7}\ rad/s$, about 4 order of magnitude lower). Difficulties arise when trying to control asteroid rotation using the laser due to:

1. the lack of knowledge of inertial properties of the body, which reduces the system capability to predict how the asteroid will behave under the control momentum;
2. the thrust alignment with the local normal to the asteroid surface where the laser is pointing, which could produce an undesired control momentum;
3. the spacecraft configuration for which the spacecraft will be able to control the rotation only around two directions.

On the contrary before the deflection operations begin, the on-board system will construct a map of the asteroid determining the regions of the asteroid where the laser will produce desired torques. Moreover the wide angle navigation camera together with the LIDAR will be used to determine the instantaneous angular rate, by tracking few feature points. Also the relative attitude could be obtained but the objective here is to reduce angular rate, not to maintain the asteroid in a fixed attitude. (The latter will require a strict control which is not possible with a fixed spacecraft configuration). .

The only information from the on board system is the estimated angular velocity relative in the Hill reference frame through image processing. In this way a control torque proportional to the angular velocity component can be determined as :

$$\mathbf{M}_{c-I} = \mathbf{r} \times \mathbf{T}_{Laser} = -k \frac{\boldsymbol{\omega}_I}{\left\| \boldsymbol{\omega}_I \right\|} \qquad [14]$$

where M_{c-I} and $\boldsymbol{\omega}_I$ are the control torque and the angular velocity in the inertial frame. For simplicity, given that the angular velocity of the Hill reference frame is very low compared to the rotations of the asteroid, the inertial frame IJK as in Fig.4 is assumed to be coincident with the Hill reference frame of xyz components. k is a scaling factor for which the magnitude of the control momentum is realizable by the system. If one does not scale the angular velocity, the desired arm could be outside of the asteroid volume. For this reason k has been defined as:

$$k = M_{asteroid} \left\| \mathbf{a}_{laser}^{estimated} \right\| \cdot r_{\max-arm} \qquad [15]$$

where $r_{\max-arm}$ is the maximum arm with respect to the CoM at a certain time. It has been assumed that the CoM is precisely known (which can be determined before starting operations). In this way even if the asteroid is rotating, the laser will always hit the surface. In components:

$$\begin{aligned} M_{c-x} &= -T_z r_y + T_y r_z \\ M_{c-y} &= T_z r_x - T_x r_z \\ M_{c-z} &= -T_y r_x + T_x r_y \end{aligned} \qquad [16]$$

In order to derive the target point on the surface of the asteroid to generate the desired control torque, one can start from considering that the spacecraft is flying along y-axis, and that the laser can be controlled only in azimuth and elevation. The azimuth and elevation of the laser beam translate into a coordinate in the x-z plane. Furthermore, it is desirable to produce a deflection action mainly along the y direction. Hence, iIn order to reduce any thrust component in the z direction the target region has been restricted to a maximum distance from y equal to 2/3 of the minor inertia axis of the asteroid.

Figure 4 sketches the proposed target point and control technique.

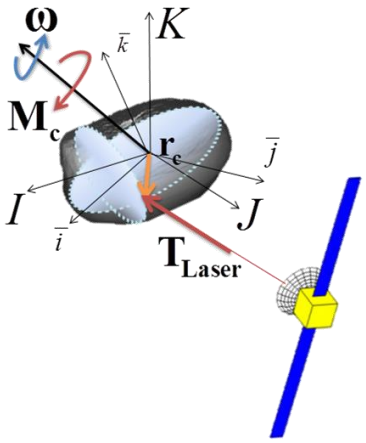

Figure 4: Angular velocity control scheme

Given these assumptions, the desired arm is given by

$$\begin{aligned} M_{c-x} / -T_y &= r_z \\ r_y &= 0 \\ M_{c-z} / T_y &= r_x \end{aligned} \qquad [17]$$

The desired arm is, thus, defined in the x-z plane.

$$\begin{aligned} \left\| \mathbf{a}_{laser}^{estimated} \right\| \cdot r_{\max-arm} \omega_{c-x} &= r_z \\ r_y &= 0 \\ \left\| \mathbf{a}_{laser}^{estimated} \right\| \cdot r_{\max-arm} \omega_{c-z} &= r_x \end{aligned} \qquad [18]$$

In this way it is not necessary to know the asteroid mass but one can rely only on the estimated angular velocity and total perturbative acceleration from the laser. To model interaction fully, one needs to identify the intersection between the line connecting the desired arm to the laser whose position is assumed to be, for simplicity, coincident with the spacecraft barycentre. Figure 5 schematically shows how the model identifies the point where the laser hits the surface and the correspondent actual control arm and thrust.

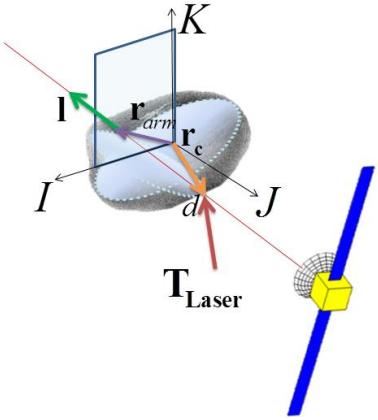

Figure 5: Spacecraft-asteroid interaction

In the following, the actual laser-asteroid interaction is explained. With reference to Figure 5, the equation of the line is given by Eq. [19]

$$\mathbf{x} = \mathbf{r}_{arm} + d\mathbf{l} \quad [19]$$

where $\mathbf{r}_{arm} = [r_x \quad r_y \quad r_z]'$ is the desired arm as defined in Eq.[17], $\mathbf{l}$ is the unit vector aligned as the spacecraft-arm direction, d is the intersection with the surface. The surface of the ellipsoid is defined as in Eq.[20]:

$$\mathbf{x}'\mathbf{A}(t)\mathbf{x} = 1 \quad [20]$$

where is given by the rotation of the ellipsoid with time:

$$\mathbf{A}(t) = \mathbf{R}(t)'\mathbf{A}_0\mathbf{R}(t) \quad [21]$$

The matrix $\mathbf{A}_0 = diag([a \quad b \quad c]^{-2})$ is assumed to be diagonal, which means that the ellipsoid axes are aligned with the inertial reference frame. $\mathbf{R}(t)$ is the asteroid rotation matrix, given by:

$$\mathbf{R}(t) = \begin{bmatrix} q_1^2 - q_2^2 - q_3^2 + q_4^2 & 2(q_1q_2 + q_3q_4) & 2(q_1q_3 - q_2q_4) \\ 2(q_1q_2 + q_3q_4) & -q_1^2 + q_2^2 - q_3^2 + q_4^2 & 2(q_2q_3 + q_1q_4) \\ 2(q_1q_3 - q_2q_4) & 2(q_2q_3 + q_1q_4) & -q_1^2 - q_2^2 + q_3^2 + q_4^2 \end{bmatrix} \quad [22]$$

By substituting Eq. [19] in Eq.[20] the intersection with the ellipsoid is defined by the solution of a second degree system of equation:

$$d^2\mathbf{l}'\mathbf{A}(t)\mathbf{l} + 2d\mathbf{l}'\mathbf{A}(t)\mathbf{r}_{arm} + (\mathbf{r}_{arm}'\mathbf{A}(t)\mathbf{r}_{arm} - 1) = 0 \quad [23]$$

Eq. [23] leads to finding two values of d :

$$d = \frac{-\mathbf{l}'\mathbf{A}(t)\mathbf{r}_{arm} \pm \sqrt{(\mathbf{l}'\mathbf{A}(t)\mathbf{r}_{arm})^2 - \mathbf{l}'\mathbf{A}(t)\mathbf{l}(\mathbf{r}_{arm}'\mathbf{A}(t)\mathbf{r}_{arm} - 1)}}{(\mathbf{l}'\mathbf{A}(t)\mathbf{l})^2} \quad [24]$$

Only the solution which gives the shortest distance between the asteroid and the spacecraft is considered. From the solution of [13], the normal to the surface, and thus the direction of exerted thrust, can be calculated. For an ellipsoid, the normal vectors are given by the gradient of the surface function as follows:

$$\mathbf{n} = \nabla(\mathbf{x}'\mathbf{A}(t)\mathbf{x} - 1) \Big/ \left\| \nabla(\mathbf{x}'\mathbf{A}(t)\mathbf{x}) \right\| = \left[\frac{x}{a^2} \quad \frac{y}{b^2} \quad \frac{z}{c^2} \right] \Big/ \left\| \left[\frac{x}{a^2} \quad \frac{y}{b^2} \quad \frac{z}{c^2} \right] \right\| \quad [25]$$

Once the normal is available the actual applied torque can be calculated by

$$\mathbf{M}_c = (\mathbf{r}_c \times \mathbf{T}_{laser}) \quad [26]$$

V. Measurements model

On board orbit determination at the asteroid will be performed by combining optical measurements from the camera with the ranging information from the laser range finder [9]. The measurements then are processed by an unscented Kalman filter selected for its capability to not introduce approximations due to linearization as the extended Kalman filter[10].The measurements from the camera are defined on the screen of the camera itself as the coordinates of the asteroid centroid and translated into angular measurements. The definition of the asteroid as seen from the camera a certain number of points are taken the asteroid surface. The position of each point is given in the spacecraft reference frame as:

$$\mathbf{x}^i_{Surf-SC} = \delta\mathbf{r}_{SC} - \mathbf{x}^i_{surface} \quad [26]$$

where $\mathbf{x}^i_{surface}$ are the vector position of the points with respect to the centre of the asteroid. Then these points are given in the camera reference frame in the components $(x_{cam}, y_{cam}, z_{cam})^i$:

$$\begin{aligned} x^i_{cam} &= \mathbf{x}^i_{Surf-SC} \cdot \mathbf{x}_{camera} \\ y^i_{cam} &= \mathbf{x}^i_{Surf-SC} \cdot \mathbf{y}_{camera} \\ z^i_{cam} &= \mathbf{x}^i_{Surf-SC} \cdot \mathbf{z}_{camera} \end{aligned} \quad [26]$$

where $\mathbf{x}_{camera}$, $\mathbf{y}_{camera}$ and $\mathbf{z}_{camera}$ represent the axes of the local camera frame. Being $\mathbf{v}^i = \begin{bmatrix} v^i_x & v^i_y & v^i_z \end{bmatrix}$ the normalized the local vector, the position of the surface point in terms of pixel can be defined as:

$$\begin{aligned} x^i_{screen} &= v^i_x t_c / p_{width} \\ y^i_{screen} &= v^i_y t_c / p_{width} \end{aligned} \quad [26]$$

where $t_c = f / v^i_z$, f is the focal length and p_{width} is the pixel width. The centroid coordinates (x_c, y_c) is obtained by the mean position of the all points on the screen of the camera. A representation of this stage of the process is reported in Figure 6 which reports also the position of the centroid with respect to the actual centre.

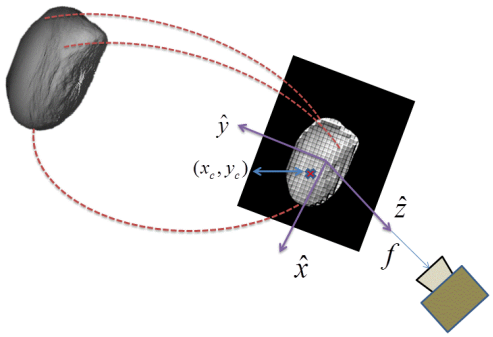

Figure 6. Centroid identification

The local azimuth and elevation angles are obtained as:

$$\theta = \tan^{-1}\frac{x_c}{f}$$

$$\varphi = \tan^{-1}\frac{y_c}{\sqrt{x_c^2 + f^2}} \quad [26]$$

The measurements from the camera results in being affected from both attitude and pixelization errors. The

latter is due to the fact that the surface points in terms of pixel are defined as multiple of pixels and could lead to mis-identifying the actual pixel position on the camera screen. A minimum of two points on the asteroid surface is necessary to make navigation system observable. When a range measurement is added to a camera image, only one visible surface point is required for the navigation system to be observable. The measurements from the LRF are given by the distance between the spacecraft and the spot the camera is pointing to:

$$d = \left| \mathbf{x}_{sc} - \mathbf{x}_{surface} \right| \qquad [26]$$

where $\mathbf{x}_{surface}$ is the position of the spot on the asteroid surface.

An impact sensor and spectrometer are embarked are used to characterize the composition of the asteroid and measure the mass flow from the ablation process. These sensors provide the system with information on the mean velocity and mass flow per unit area of the ejecta plume. These can be used to estimate the force exerted by the ejecta plume as:

$$F_{plume} = \dot{m}_{laser} \bar{v} A(attitude) \qquad [26]$$

where $\dot{m}_{laser}$ is the mean mass flow per unit area, $\bar{v}$ is the mean ejection velocity and $A(attitude)$ is the cross section of the spacecraft with respect to the ejection velocity (which depends on the attitude).

V.II Optical Flow

In order to control the asteroid rotation rates, it is necessary to estimate its instantaneous angular velocity. Tracking feature points of the asteroid can be used in an efficient implementation to characterize the asteroid's rotational state. Two methods can be used proposed to perform the asteroid's rotational state determination. The first method, the Fourier Spectral analysis method, reconstruct the rotation of the asteroid by performing a Fourier analysis of the movement of selected features on the surface of the asteroid. The Fourier Spectral analysis methods works applies a fast Fourier Transform (FFT) to a batch of measurements over a period of time sufficiently long to capture the lower desirable rotational frequencies[11]. The second method is based on the optical flow method to extract rotation information by tracking the movement of selected features on the surface of the asteroid. The method can be used to estimate the instantaneous rotation of the asteroid. Both method rely on the feature extraction algorithm and can be implemented on-board to autonomously control the rotation of the asteroid during deflection. This FFT method assumes that the asteroid's motion is described by the superposition of the rotations with constant angular velocities. Using the combination of camera, ranging instruments, and model of the asteroid, the estimator can obtain three dimensional position information of the points on the object. From these measurements, it can estimate the rotational parameters of the asteroid - each frequency and direction of the axes of rotation can be computed by applying a Fourier transform to a time sequence of the points' three dimensional positions. This method has been envisaged for debris capture and removal missions, and works on the premises that the motion is free torque force acting on the body and characteristic frequencies of rotation are distinct [11]. The main drawbacks are represented by the fact the method is suitable especially for symmetric bodies and that a batch of measurements needs to be processed over long time to identify lowest frequencies correctly. Conversely, the optical flow method has been already employed and it is being used on the Rosetta mission during landing[12], where it is critical to determine the relative attitude and position with respect to the surface, possibly integrating imaging information with the range measurements from radar or LIDAR. Feature points have specific characteristics that makes them distinguishable from others in their surroundings. Knowing how points evolve in the image frame, the velocities and angular rates with respect to the camera can be deduced.

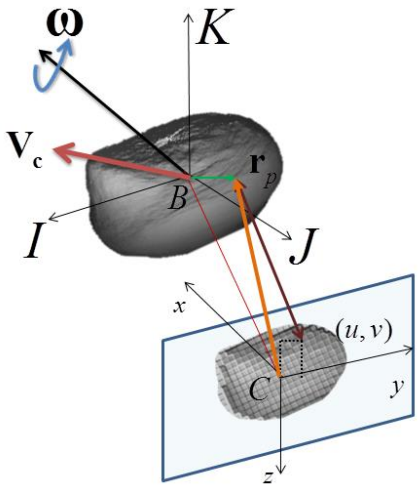

Figure 7. Pin-Hole Camera Model

To extract the velocity from the feature point, the "*pinhole*" model of a camera is used [13]:

$$\begin{bmatrix} u \\ v \end{bmatrix} = \frac{f}{x_c} \begin{bmatrix} y_c \\ z_c \end{bmatrix} \qquad [27]$$

where (u,v) is the projection in the focal plane of the camera; $\mathbf{r_c} = [x_c \quad y_c \quad z_c]$ is the position of the point in the camera reference frame; x_c is the distance in the

boresight direction and f the focal length of the camera.

Applying the time derivative to both sides of the pin-hole camera model, it is possible to relate the optical flow with the angular and linear velocity of the asteroid:

$$\begin{bmatrix}\dot{u}\\ \dot{v}\end{bmatrix}=\frac{f_c}{x_c}\begin{bmatrix}\frac{dy_c}{dt}\\ \frac{dz_c}{dt}\end{bmatrix}-\frac{f_c}{x_c^2}\frac{dx_c}{dt}\begin{bmatrix}y_c\\ z_c\end{bmatrix}$$

$$\begin{bmatrix}\frac{dx_c}{dt} & \frac{dy_c}{dt} & \frac{dz_c}{dt}\end{bmatrix}=-{}^c\boldsymbol{\omega}_{B/C}\times\mathbf{r_c}-{}^c\mathbf{V}_{B/C} \quad [27]$$

Substituting the second equation in Eq.23 and reorganizing it to make it a function of $\mathbf{V}_{B/C}$ and $\boldsymbol{\omega}_{B/C}$, which are respectively the linear and angular velocities of the body relative to the camera :

$$\begin{bmatrix}\dot{u}\\ \dot{v}\end{bmatrix}=M(f,c_p)\begin{bmatrix}{}^cV_{B/C}\\ {}^c\omega_{B/C}\end{bmatrix} \quad [28]$$

$$M(f,c_p)=\begin{bmatrix}-\frac{u}{x_c} & \frac{f}{x_c} & 0 & -v & -\frac{uv}{f} & \frac{u^2}{f}+f\\ -\frac{v}{x_c} & 0 & \frac{f}{x_c} & u & -\frac{v^2}{f}-f & \frac{uv}{f}\end{bmatrix} \quad [28]$$

Eqs. [28] and [28] lead to a representation of the motion of the points with respect to the camera frame, including the angular velocities. Anyway by using the position of the points on with respect to the asteroid centre of gravity, a different form of Eq. [28] can be obtained:

$$M(f,c_p)=\begin{bmatrix}-\frac{u}{x_c} & \frac{f}{x_c} & 0 & -v & -\frac{uv}{f} & \frac{u^2}{f}+f\frac{x_c^a}{x_c}\\ -\frac{v}{x_c} & 0 & \frac{f}{x_c}rr & u & -\frac{v^2}{f}-f\frac{x_c^a}{x_c} & \frac{uv}{f}\end{bmatrix} \quad [28]$$

where x_c^a is the distance of the feature point to the centre with respect to the boresight direction. Adding the information from other feature points and pseudo-inverting, both $\mathbf{V}_{B/C}$ and $\boldsymbol{\omega}_{B/C}$ are directly calculated.

$$\begin{bmatrix}{}^c\mathbf{V}_{B/C}\\ {}^c\boldsymbol{\omega}_{B/C}\end{bmatrix}=\begin{bmatrix}M(f,c_{P_1},c_{O_B})\\ \vdots\\ M(f,c_{P_N},c_{O_B})\end{bmatrix}^+\begin{bmatrix}\dot{u}_1\\ \dot{v}_1\\ \\ \dot{u}_N\\ \dot{v}_N\end{bmatrix} \quad [29]$$

where the $+$ sign stands for pseudo-inverse. The algorithm allows extracting velocity and attitude rates from at least 3 tracked feature points from two consecutive frames.

- No approximations are done in this model. However, $\dot{u}$ and $\dot{v}$ are not available, so they are replaced by $\Delta\mathbf{u}/\Delta t$. This is to assume that this value is small, which should be the case considering the camera extracts 10 FPS and the fastest rotation rate should be 19/hour.
- The equations are linear with respect to the evaluated variations of the feature points ($\dot{u}$, $\dot{v}$). The matrix, however, depends on a value that cannot be directly measured by the camera, the distance to the boresight direction to each of the points. So the information from the camera needs to be complemented using the model of the asteroid's surface.
- Relative velocity can be extracted from navigation filter so the algorithm can be adapted. Rearranging the equations:

$$\begin{bmatrix}\dot{u}\\ \dot{v}\end{bmatrix}=\begin{bmatrix}-\frac{u}{x_c^e} & \frac{f}{x_c} & 0\\ -\frac{v}{x_c^e} & 0 & \frac{f}{x_c^e}\end{bmatrix}{}^cV_{B/C}^e+\begin{bmatrix}-v & -\frac{uv}{f} & \frac{u^2}{f}+f\frac{x_c^{a-e}}{x_c^e}\\ u & -\frac{v^2}{f}-f\frac{x_c^{a-e}}{x_c^e} & \frac{uv}{f}\end{bmatrix}{}^c\omega_{B/C}^e \quad [29]$$

where the apex *e* refers to the estimated quantities. Thus obtaining:

$${}^c\omega_{B/C}^e=\begin{bmatrix}-v & -\frac{uv}{f} & \frac{u^2}{f}+f\frac{x_c^{a-e}}{x_c^e}\\ u & -\frac{v^2}{f}-f\frac{x_c^{a-e}}{x_c^e} & \frac{uv}{f}\end{bmatrix}^{-1}\left(\begin{bmatrix}\dot{u}\\ \dot{v}\end{bmatrix}-\begin{bmatrix}-\frac{u}{x_c^e} & \frac{f}{x_c^e} & 0\\ -\frac{v}{x_c^e} & 0 & \frac{f}{x_c^e}\end{bmatrix}{}^cV_{B/C}^e\right) \quad [30]$$

Finally $\boldsymbol{\omega}_{I-e}$ for Eq. [14]is obtained by rotating ${}^c\omega_{B/C}^e$ from the camera frame to the asteroid frame. Through this method, at each time a batch of points are processed, an estimate of the rotation rate of the asteroid with respect to the camera is obtained (the attitude and rotation rate of the camera is well known from the spacecraft attitude determination). The method is affected by errors coming from the identification of the features on the surface (pixelization error), as well as the spacecraft position error from the translational filter. As an example reports the error of the optical flow system during 14 days operations. A number of 10 features have been considered at each time.

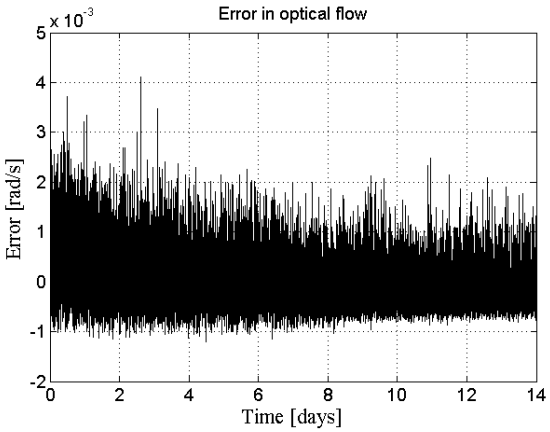

Figure 8: Optical Flow error

In general the system is able to determine the angular rate as precise as few milliradians per second.

VI ACCELERATION ESTIMATE

During operations it is vital to measure the effectiveness of the momentum coupling. The on-board GNC system is able to determine the relative acceleration between the spacecraft and the asteroid. The effect of the thrust exerted by the laser ablation produces a dragging force whose effect is coupled with the plume impingement. The impact sensor gives the necessary information on the mass flow and velocity of the ejecta acting on the direction normal to the surface facing the plume. The contribution of the plume is not negligible The premise of this method is that we can rely on precise methods to model the effects from the laser recoil and from the solar radiation pressure. This is the case, because the acceleration from the solar pressure can be filtered and precise estimated will be available during ground station campaign. Moreover during calibration, the laser recoil will be estimated precisely by simply firing the laser in the asteroid direction defocusing the beam, so that it will not produce any laser ablation. The proposed method consist of augmenting the state variable the on board system needs to estimate during laser operations, by two variables, which represent the dragging force due to the laser ablation and the plume impingement acceleration. In this way the variables, which the filter will need to estimate, are $[x, y, z, v_x, v_y, v_z, \mathbf{a}_{laser}, a_{plume}]$. The approach is the one used to estimate biases, commonly used to estimate solar radiation pressure[14]. The dynamics equations associated to the acceleration from the laser ablation and the plume impingement is thus time independent:

$$\begin{aligned} \dot{\mathbf{a}}_{laser} &= 0 + \mathbf{v}_{laser} \\ \dot{a}_{plume} &= 0 + \nu_{plume} \end{aligned} \qquad [30]$$

where $\mathbf{v}_{laser}$ and ν_{plume} are system noises, which means that the dynamics of these variables is driven by the noises. It has been assumed that the force from the plume is exerted along the asteroid-spacecraft direction. The acceleration from laser is used to update both the spacecraft and the asteroid dynamics in Eqs. and [4]. It has been hereafter considered the level of noise on the system equal to the 10% of the nominal value. Treating these accelerations as biases is a strong assumption because it implies that their dynamics is slowly varying with time. However, by keeping the spacecraft within a small control box, one can maintain the acceleration almost constant, thus limiting the dynamics effects from the laser ablation.

VII. RESULTS

Following the study[4], it has been assumed to use the near Earth object 2006 RH120 whose characteristics are listed in Table 1.

Orbital Elements at Epoch 2456200.5 (2012-Sep-30.0) TDB
Reference: JPL 45 (heliocentric ecliptic J2000)

Element	Value	Uncertainty (1-sigma)	Units
e	.0244740306228480 1	4.2401e-05	
a	1.033252056035198	1.0251	AU
q	1.007964213574672	1	AU
i	.5952660003048117	9.4379e-05	deg
node	51.14334927580387	3.8304e-05	deg
peri	10.14353817485877	0.092984	deg
M	221.2498016727181	206.48	deg
t_P	2456348.356001016605 (2013-Feb-24.85600102)	1	JED
period	383.6258326667335	570.89	d
	1.05	1.563	yr
n	.9384143854377558	1.3965	deg/d
Q	1.058539898495724	1.0502	AU

Table 1. Orbital elements and physical characteristics of 2006 RH120 (http://ssd.jpl.nasa.gov/sbdb.cgi?sstr=2006%20RH120),

This is a small rocky asteroid with an estimated mass of 130 tonnes. The laser ablation starts when the asteroid is at perihelion. The initial angular velocity is [0.0052 0.0052 0.0332]rad/s. At the beginning of operations the asteroid principal axes of inertia are aligned to the Hill's frame axes. This means that the spacecraft is assumed to rotate mainly along the z-axis at the beginning of the operations with smaller components on the other 2 axis. The inertial matrix is assumed to be almost diagonal, as given for an ellipsoid with extra-diagonal components equal to 1% of the minimum axis inertia. Since the overall process is stochastic, the random process has been seeded to produce the same results for both the discrete and continuous control. The results, hereafter reported, simulates operations at the asteroid for 14 days.

VII.I Estimated and Controlled Motion

The on-board system estimates the relative trajectory of the spacecraft. As one can see from Fig.9 and Fig.10,

the filter produces similar performance in both the discrete and continuous control.. The estimate is as precise as 20 cm in position and less than 0.1 mm/s.In general the maximum error is on the y-axis.

The most noticeable difference is due to the fact that in the case of the continuous control the number of peaks with maximum error (circa 20 cm) is higher than in the case of discrete control. Conversely when one considers the actual error with respect to the desired position (i.e. spacecraft placed with zero velocity at 50 m along track with), the continuous control maintains the spacecraft closer to the desired trajectory as shown in Fig.12 with maximum error in the range of 40 cm in position and 0.1mm/s. On the contrary Fig.11 shows that the discrete control sometimes fails to maintain the spacecraft within 0.5m. Moreover as shown in Fig.11.b, the maximum error in velocity is up to 4 times higher than the former case.

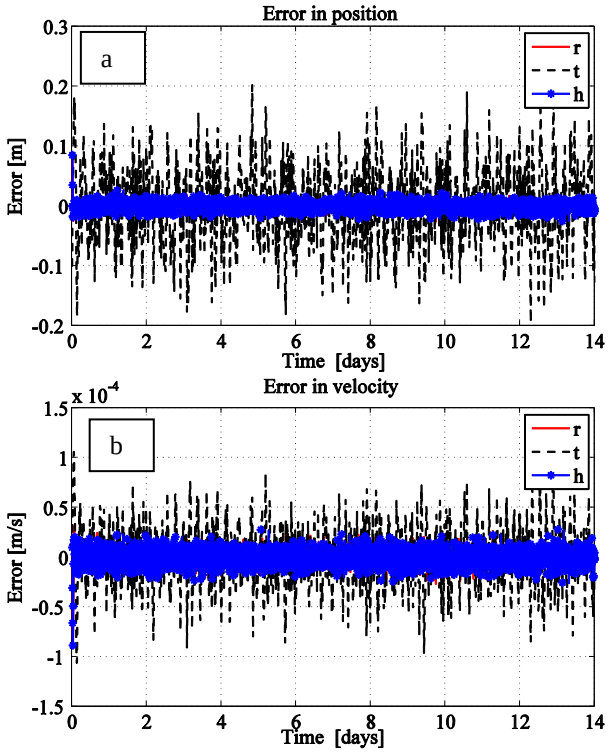

Figure 9: Discrete Control -Estimated position(a) and velocity error(b).

The reason for these trends can be easily explained. The discrete control allows the spacecraft to move freely within the control box. During this phase the estimate is less affected by the noise introduced by the measurements into the dynamics through the control. Then the peaks outside the control box are due to the fact that the control logic works when the estimated position is outside the control box. Given the error in the estimated trajectory, the spacecraft is actually maintained within a 80 cm control box.

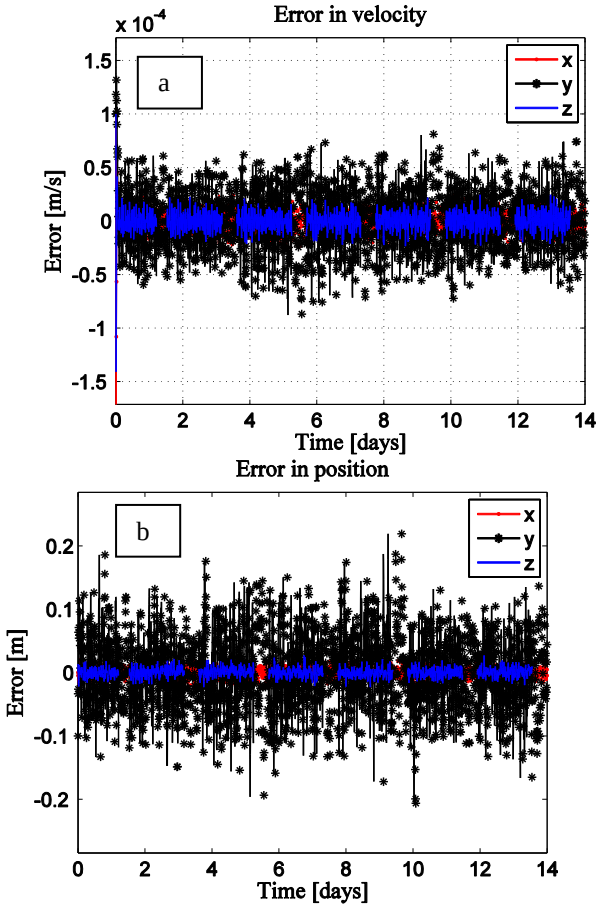

Figure 10: Low Thrust Control -Estimated position (a) and velocity error (b).

Anyway in both cases, the controller uses also the estimated accelerations which is affected by high level of noise. This leads sometimes to apply higher or lower level of control with subsequent peaks in the position or velocity.

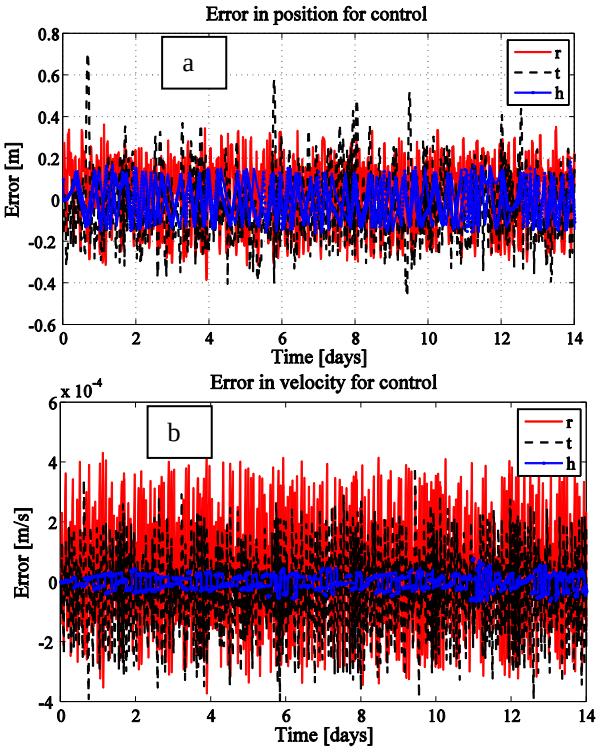

Figure 11: Discrete Control - Actual controlled position (a) and velocity error (b).

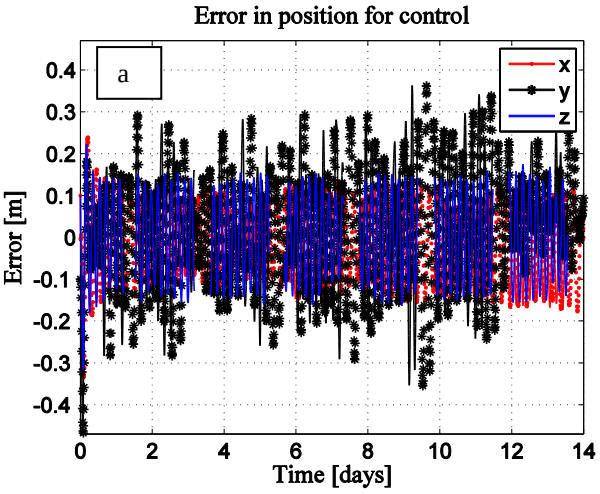

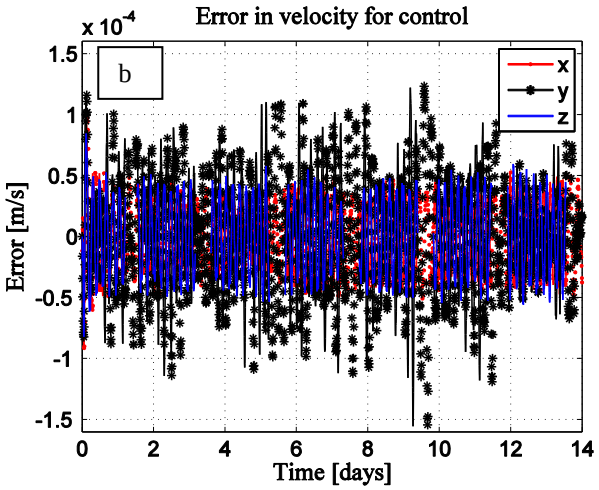

Figure 12: Low Thrust Control - Actual controlled position (a) and velocity error (b).

VII.II Asteroid Control

Implementing the method described Section III.III the rotational velocity is progressively decreased. Fig.13 reports the set of points representing the projection of the control arm on the x-z plane for the asteroid for the discrete case (the continuous one is very similar). The distance of each points from the centre of mass is about 1 m, which is 2/3 or the minor axis. Since the main component of the rotation is along the z-axis, the control arm has as major components along x-axis for the selected period of time.

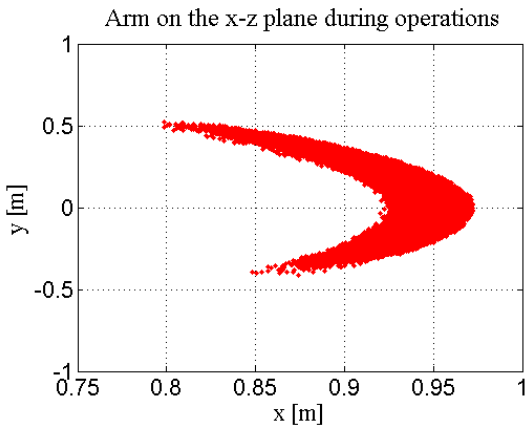

Figure 13 - Typical distribution for the desired control arm on the x-z plane during 14 days operations.

As one can see from Fig.14, the magnitude of the angular velocity decreases with time in both the implemented control strategies. Small oscillations are present in the first days of operations.

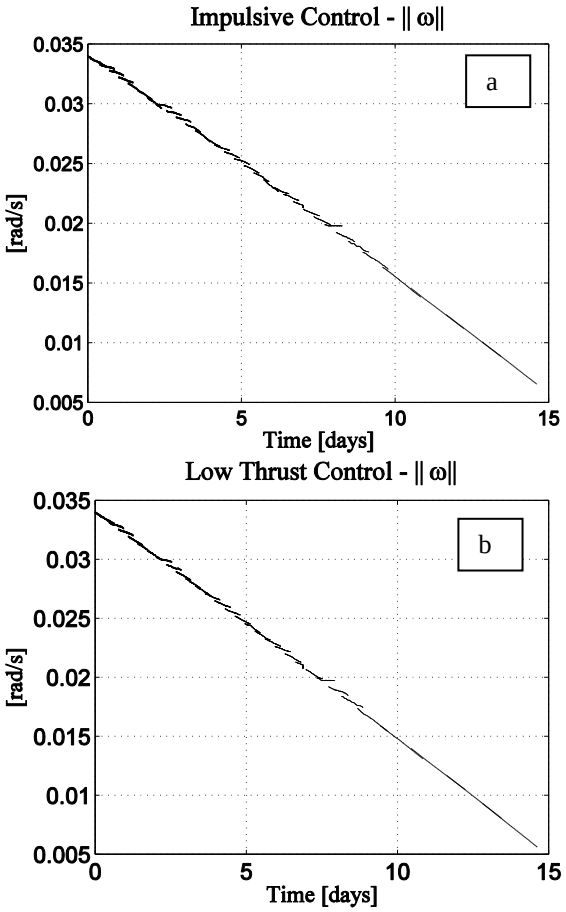

Figure 14: Controlled angular velocity for discrete (a) and continuous (b) control.

Although similar, the two curves have slightly different slope. In particular, the continuous control strategy reaches 0.01 rad/s after 12.46 days of de-spinning operations while the discrete control takes about 12.85 days to reach the same value, although both control were affected by the same statistical errors in the measurements. This descends directly from the fact the former control is more precise, and this means the thrust levels, thus the control torques, are higher than in the discrete case.

VII.III Estimated Deflection Action

Last results presented regard the estimated perturbations. As shown in Fig.15 and Fig.16, as expected the the trend is very similar for the implemented control strategy.

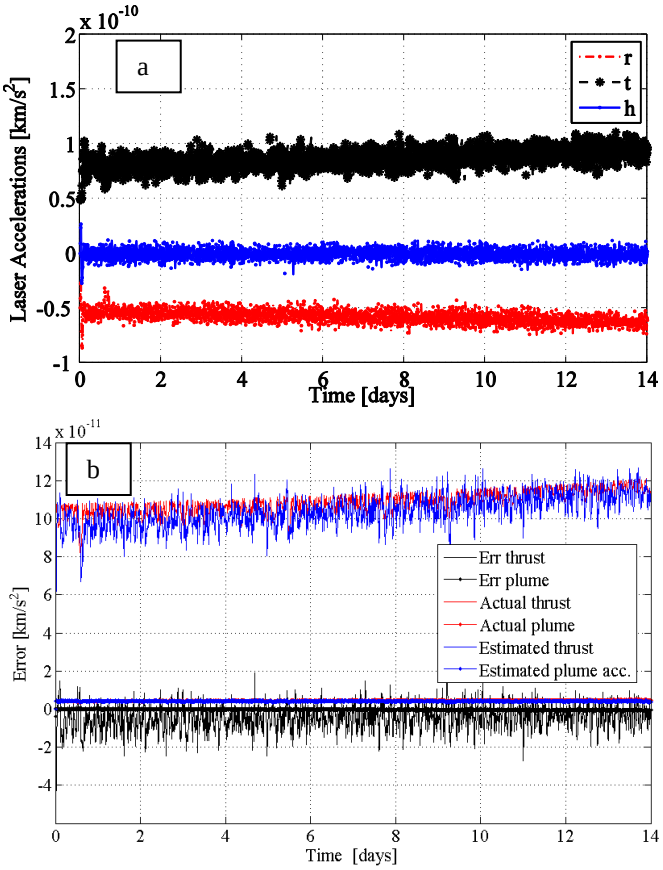

Figure 15: Discrete Control - Estimated acceleration from the laser (a) and acceleration from the laser and plume force vs. the actual forces (b)

As in the case of the angular velocity in Section V.II, the difference resides in the slope of the curve. Also in this case, this is due to the fact that a finer control produces better focussing accuracies with higher control torque. This causes the asteroid to slow down in relatively less time, increasing the efficiency of the ablative process. For the same reasons the error peaks are smaller in the case of continuous thrust.

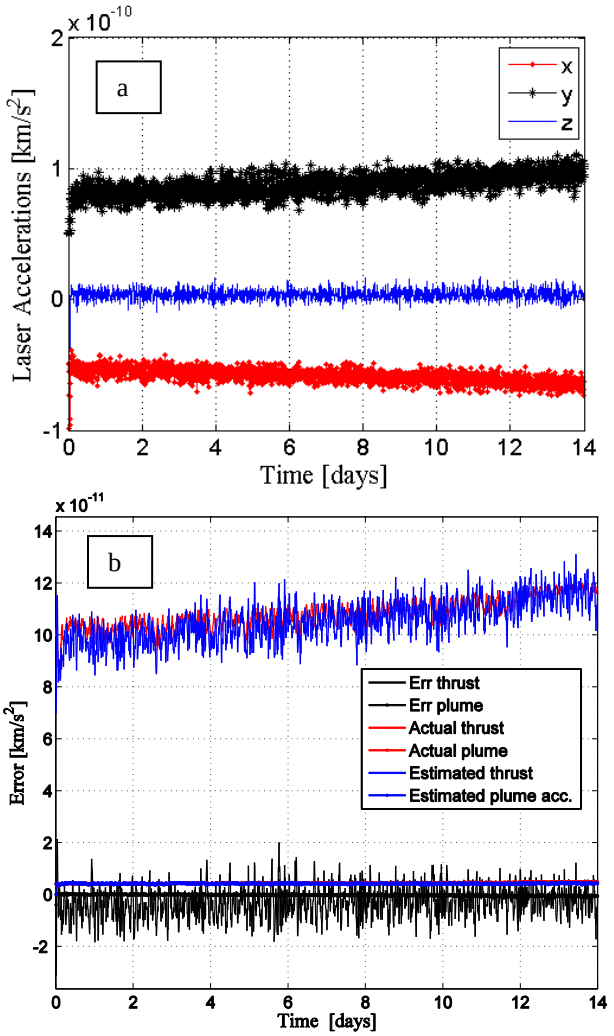

Figure 16: Low Thrust Control - Estimated Estimated acceleration from the laser (a) and acceleration from the laser and plume force vs. the actual forces (b)

The advantage of this method is that there is no assumption on the laser ablation model, which requires the knowledge of a complex dynamics model, involving asteroid kinematics and composition, reaction thermodynamics, a number of variables which cannot be drawn from the embarked payload.

VIII.CONCLUSIONS

This paper presented an autonomous GNC for asteroid deflection and attitude control via laser ablation. In order to maintain the optimal focussing of the laser, a precise GNC system is required to control the spacecraft at a given distance from the asteroid. Discrete and continuous control methods have been considered for this task. Both methods are based on on-board estimates of position, velocity and perturbative accelerations from the ablative process. Camera and ranging instruments are used to estimate the spacecraft relative motion, while additional information from an impact sensor and spectrometer is used to separate the plume impingement contribution from the actual acceleration due to the laser ablation. In this way the deflection action on the asteroid could be estimated without relying on any interaction model between the laser and the asteroid.

This paper demonstrates that laser ablation can be employed to reduce angular velocity of the asteroid by pointing the laser off-barycentre. Without relying on the inertial characteristics, except for the knowledge of the centre of mass, it has been shown that it is possible to decrease asteroid's spin rate, when the asteroid is a compact ellipsoid and rotates mainly along the out-of-plane direction. In this paper the region where the laser can be pointed has been restricted such that the thrust is almost contained in the orbital plane. This does not produce the maximum achievable control torque but provide a deflection action in the desired direction. Future works will consider asteroids with irregular shape (i.e. ellipsoid with higher curvature) and methods to maximise the desired torque accordingly.

Finally, from the experiments in this paper one could observe that the continuous control decreases the asteroid rotation rate in less time than the discrete control. The reason for this faster de-spinning can be found in the more precise control which maintains a better focusing of the laser

---

1 http:// neo.jpl.nasa.gov/stats

2 Colombo, C., Sanchez Cuartielles, J. P., Vasile, M., Radice, G., October 2006. A comparative assessment of different deviation strategies for dangerous NEO. In: International Astronautical Congress. Valencia, Spain.

3 Melosh, H. J., Nemchinov, I. V., Zetzer, Y. I., 1994. Non-nuclear strategies for deflecting comets and asteroids. In: Gehrels, T. (Ed.), Hazard due to comets and asteroids. University of Arizona Press, pp. 1111–1132.

4 Vasile M., Vetrisano M., Gibbings A., Garcia Yarnoz D., Sanchez Cuartielles J-P., Burns D., Hopkins J-M., Colombo C., Branco J., Wayman A., Eckersley S., Light Touch2, Effective Solutions to Asteroid Manipulation, February 2013.

5 Kahle, R., Kuhrt, E., Hahn, G., Knollenberg, J., 2006. Physical limits of solar collectors in deflecting Earth-threatening asteroids. Aerospace Science and Technology 10, 253–263.

[6] Hu, W. and Scheeres, D. J., July–August 2002. Spacecraft motion about slowly rotating asteroids. Journal of Guidance, Control and Dynamics 25 (4), 765–775.

[7] Schaub, H. and Junkins, J. L., 2003. Analytical mechanics of space systems, 1st Edition. AIAA Education Series. AIAA, Virginia, U.S.A.

[8] Vasile, M. and Maddock, C.A., 2011: Design of a Formation of Solar Pumped Lasers for Asteroid Deflection, Preprint submitted to Advances in Space Research

[9] Dionne, K., 2009 : Improving Autonomous Optical Navigation for Small Body Exploration Using Range Measurements. AIAA 2009-6106. AIAA Guidance, Navigation, and Control Conference, 10 - 13 August 2009, Chicago, Illinois

[10] Julier, J., Uhlmann, K. and Durrant-Whyte, H.F., 1995: A new approach for filtering nonlinear systems, Proceedings of the American Control conference, Seattle, Washington.

[11] Hiroaki Hirai, Yasuhiro Masutani, Fumio Miyazaki, 1998: Motion Estimation of an Unknown Rigid Body Rotating Freely in Zero Gravity Based on Complex Spectrum of Position of a Point on the Body, IEEE International Conference on Robotics & Automation Leuven, Belgium, May 1998.

[12] Gil-Fernandez, J., 2012: Autonomous GNC System to enhance science of asteroid. 63rd International Astronautical Congress, Naples, Italy.

[13] Johnson, A.E. and Matthies, L. H. Precise Image-Based Motion Estimation for Autonomous Small Body Exploration. Appearing in the 5th International Symposium on Artificial Intelligence, Robotics and Automation in Space (iSAIRAS'99), pp. 627-634.

[14] Maybeck, Peter S. (1979). Stochastic Models, Estimation, and Control. Mathematics in Science and Engineering. 141-1. New York: Academic Press. pp. 423. ISBN 0-12-480701-1.